

UNIVERSITY OF BRITISH COLUMBIA

COMPREHENSIVE EXAM REPORT

---

**Molecular Dynamics Simulations of  
Heterogeneous Ice Nucleation by  
Atmospheric Aerosols**

---

*Author:*

Stephen ZIELKE

*Supervisors:*

Dr. Allan BERTRAM

Dr. Gren PATEY

*Chair:*

Dr. Leslie BURTNICK

*Committee:*

Dr. Keng CHOU

Dr. Yan Alexander WANG

Dr. Michael WOLF

1:00-3:30pm Wed. April 9, 2014  
Chemistry D317

## 1 Introduction

Aerosols play an important role in the atmosphere affecting earth's climate, weather and human health. Aerosols can come from a variety of natural and anthropogenic sources and range in size from 1nm to 10 $\mu\text{m}$ [1]. Aerosols can be grouped into two main classes based on their interaction with water: cloud condensation nuclei that allow water to condense into clouds and ice nuclei (IN) that freeze water at temperatures above -38°C.

Although a common process, the freezing of water is still an area of research receiving a lot of attention[2]. Water melts at 0°C, but pure water droplets will not freeze until -38°C[3]. Water can freeze at higher temperatures with the aid of a heterogeneous IN[1] that acts as a catalyst and lowers the Gibbs free energy of nucleation. IN form a minor component of atmospheric aerosols with estimates that approximately only 1/1000000 aerosol particles are active IN at -20°C. Yet IN play an important role in weather, for instance most rain begins as ice crystals, which grow large enough to fall, via the Bergeron-Findeisen process, where ice crystals grow at the expense of water droplets. Various requirements have been proposed to explain how atmospheric particles act as effective IN[4]: IN need to be insoluble in water, need to be larger than the critical ice embryo, able to bond to water, have one or more “active sites” capable of nucleating ice, and lastly the crystal structures of ice and the IN need to match. A mismatch between structures is quantified in equation 1,

$$\delta = \frac{n a_{o,n} - m a_{o,i}}{m a_{o,i}} \times 100\% \quad (1)$$

where the mismatch,  $\delta$ , is the percentage difference between the lattice parameters of ice,  $a_{o,i}$ , and the IN,  $a_{o,n}$ .  $m$  and  $n$  are integers which are chosen to minimize  $\delta$ . Good IN will generally have mismatches of less than a few percent.

Freezing of water initiated by an IN can occur via one of several mechanisms. Deposition freezing occurs with water vapour freezing directly onto an IN without significant liquid water forming, contact freezing occurs when a liquid water droplet encounters an IN and nucleates at its interface, and immersion freezing occurs when ice nucleation occurs on an

IN immersed inside a liquid droplet.

Classical nucleation theory (CNT) provides a general theoretical framework for nucleation of one phase of a substance into another[1, 5]. In CNT a nucleus is a sphere of a one phase in a bulk solution of the other. Monomers of the substance can then join or leave the nucleus one at a time. Thermodynamically, the Gibbs free energy of nucleation is thought of as the decrease in free energy as the nucleus forms competing against the increase due to the formation of a new interface,

$$\Delta G(a) = n_2 \frac{4\pi a^3}{3} (\Delta\mu_{1,2}) + 4\pi a^2 \gamma_{1,2} \quad (2)$$

where in the first term  $\Delta\mu_{1,2}$  is the difference in chemical potential of the bulk(1) and nucleated(2) phases, which is negative, multiplied by the volume of a sphere of radius  $a$  and the density of the nucleated phase  $n_2$ . Added to this term is the destabilization by the interface given by the area of the sphere multiplied by the interfacial free energy,  $\gamma_{1,2}$ . This equation gives rise to a critical radius,  $a^*$ , and an activation barrier,  $\Delta G(a)^*$ . A nucleus larger than the critical radius will grow spontaneously, but a smaller one will not.

There are at least sixteen polymorphs of ice[6], most of which are named with a Roman numeral indicating the order in which the polymorph was found. The most common form of ice that exists under atmospheric conditions is ice I which is usually referred to as hexagonal ice, or  $I_h$ . A metastable form of ice that can also exist under atmospheric conditions is cubic ice, or  $I_c$ . Ices II-XV are usually higher density forms of ice or proton ordered forms of other ices. Oxygen atoms in ice are well ordered and structures of ice are generally based on the arrangement of the oxygen atoms. Hydrogen atoms hydrogen bond to neighbouring water molecules, however the orientation of the water molecules is unordered, and even at 0 K there is a residual entropy.

$I_h$  and  $I_c$  are both made of of a similar layer of water molecules and differ in their stacking pattern. This layer is made of water molecules forming hexagonal rings in the chair conformation, creating two sub-layers, or a bilayer as it will be referred to in this report. Differences in the stacking of this bilayer results in different forms of ice. An ABAB... stacking pattern

gives  $I_h$  which has a hexagonal unit cell, and an ABCABC... stacking gives  $I_c$  which has a face-centred-cubic (FCC) unit cell. The difference between  $I_h$  and  $I_c$  can also be seen in the types of rings that are formed between each bilayer. In  $I_h$  the rings are boats, while in  $I_c$  chairs are formed as well[7]. Previous simulations have shown that ice prefers to grow on the bilayer[8], and the form of ice can change from layer to layer as there is a very low interfacial energy between each form of ice[9].

The goal of this project is to carry out molecular dynamics simulations of water on various IN to determine if ice can nucleate on these surfaces in simulations. If we observe ice nucleation, we will then use the simulations to provide an explanation for why some surfaces are efficient IN and others are not. To date simulations have been carried out on silver iodide and several minerals. Below we present the results of simulations on these surfaces and mention the direction of future work.

## 2 Methods

### 2.1 Molecular dynamics

To investigate the nucleation of ice on atmospheric aerosols we employ molecular dynamics simulations. Molecular dynamics is a classical treatment of molecules and atoms. Molecules and atoms interact via simple potentials and their motion is governed by Newton's equations of motion. In the simulations that are described here, the potential energy between two particles is calculated according to equation 3.

$$u_{ij}(r) = \frac{q_i q_j}{4\pi\epsilon_0 r_{ij}} + 4\epsilon \left[ \left( \frac{\sigma}{r_{ij}} \right)^{12} - \left( \frac{\sigma}{r_{ij}} \right)^6 \right] \quad (3)$$

The first term is the coulombic interaction between particles with charges  $q_i$  and  $q_j$  separated by distance  $r_{ij}$ , and  $\epsilon_0$  is the vacuum permittivity. The coulombic interaction is followed by the Lennard-Jones potential which accounts for Van der Waals forces and short range repulsion.  $\sigma$  sets the size of the particle and  $\epsilon$  sets the depth of the energy well causing short

range attraction between particles. This treatment allows for simulations of systems that are much larger than quantum mechanics based calculations. A molecular dynamics simulation involves a series of steps[10]:

1. The simulation is initialized, initial positions of particles are created and velocities are generated. Often many of the parameters for initialization are stored in several files which are read into the program, giving it the instructions needed to run the simulation.
2. Forces between each particle are calculated. Forces,  $\vec{F}(r)$ , are determined by equation 4.

$$\vec{F}(r) = \sum_{i=1}^{n-1} \sum_{j=2}^n \vec{F}(r_{ij}) \text{ where } \vec{F}(r_{ij}) = -\frac{du(r_{ij})}{d\vec{r}} \quad (4)$$

The negative of the derivative of the pair interaction energy,  $u(r_{ij})$  is summed over all pairs of particles in the simulation separated by distance  $r_{ij}$ . Due to the summation in equation 4 this step is the most time consuming part of any simulation.

3. Particles are then moved by integrating Newton's equations of motion. Several methods for doing this exist. The traditional one is the Verlet algorithm. Here the position of the particle in the subsequent time step is approximated as a Taylor expansion around its current position. Added to this expansion is another Taylor expansion of the particle's position in the previous time step resulting in equation 5,

$$x(t + \Delta t) = 2x(t) - x(t - \Delta t) + \frac{F_x(t)}{m} \Delta t^2 \quad (5)$$

where  $\Delta t$  is the time step and  $m$  is the mass of the particle. This equation does a reasonable job of conserving energy in a simulation, which is required as molecular dynamics naturally simulates systems of constant energy, and is reversible in time. The Verlet algorithm does not directly incorporate the velocity of the particles into its equation.

It is possible to derive mathematically equivalent equations that do incorporate the velocity, such as the velocity-verlet algorithm and the Leap Frog algorithm, the latter of which is used in the simulations reported here. The Leap Frog algorithm, equations 6 and 7, updates the velocity of the particle half a time step ahead of the current position, followed by the position “leaping” over the velocity to the next time step.

$$v(t + \Delta t/2) = v(t - \Delta t/2) + \Delta t \frac{F(t)}{m} \quad (6)$$

$$x(t + \Delta t) = x(t) + \Delta t v(t + \Delta t/2) \quad (7)$$

4. Steps 2 and 3 are repeated until the simulation is complete at which point data calculated during the simulation is reported or additional software is used to conduct analysis of the simulation from saved trajectories or other data. One of the primary analysis tools we use is the CHILL algorithm[11] which detects which water molecules in the simulation have frozen, and the phase of ice. The algorithm is based on analysis of the oxygen atoms of a particular water molecule and the four nearest neighbouring water molecules. If all four bonds are staggered the water is part of  $I_c$ ; if only three of the bonds are staggered and one is eclipsed the water molecule is part of  $I_h$ .

Simulations have a finite size which can cause unrealistic results. Boundaries are “removed” from the simulation to give more realistic results by means of periodic boundary conditions (PBC). Under PBC, when a particle encounters a wall of the simulation cell it disappears at that wall and reappears at the opposite wall. Force calculations are done to include periodicity as particles only interact with the nearest images of other particles.

Molecular dynamics naturally simulates a system in the microcanonical ensemble, where the number of particles, volume and energy remain constant. However, other ensembles are often desired, so thermostats and barostats are used to produce a simulation in the correct ensemble. In this report, simulations are done under canonical, constant number of particles, volume and temperature, conditions and a thermostat is used to maintain a constant average

temperature. There are several different thermostats that have been created, one of the simplest being the Anderson thermostat. This thermostat couples the simulation to a heat bath via random particles that are selected and their velocities are changed to lie within a Maxwell-Boltzmann distribution around the desired temperature. This method produces the correct ensemble for equilibrium properties of the system, however the random changing of particle velocities ruins any dynamical information, such as diffusion coefficients, that can be obtained. There are however other thermostats that produce the correct ensemble and keep the dynamics of the simulation deterministic.

One such thermostat that can produce the correct ensemble with deterministic dynamics is the Nose-Hoover thermostat[10, 12]. Here additional terms are added to the Lagrangian of the simulation to couple the simulation to a heat reservoir,

$$\mathcal{L} = \sum_{i=1}^N \frac{m_i}{2} s^2 \dot{r}_i^2 - u(r^N) + \frac{Q}{2} \dot{s}^2 - (f+1)k_B T lns \quad (8)$$

where the first and second term are the kinetic and potential energies of the real system and the third and fourth are regarded as the kinetic and potential energies of the reservoir. The potential energy of the system,  $u(r^N)$ , is a function of the positions of  $N$  particles in the system.  $m$ ,  $r$ ,  $f$ ,  $k_B$ , and  $T$  are the mass and position of a particle in the system, the degrees of freedom of the system, the Boltzmann constant and the temperature of the system respectively.  $s$  is an additional coordinate from the heat reservoir and  $Q$  determines the strength of the coupling of the system to the reservoir. Dots over variables indicate a time derivative. From equation 8 the equations of motion can be derived

$$\ddot{r} = \frac{a}{s^2} - \frac{2\dot{s}\dot{r}}{s} \quad (9)$$

$$Q\ddot{s} = \sum_i m\dot{r}_i^2 s - \frac{(f+1)k_B T}{s} \quad (10)$$

## 2.2 Simulation details

To carry out the simulations we employed the GROMACS 4.5.5 molecular dynamics software package[13] as it can easily handle large simulations. Water was represented with two different models to ensure that the results are independent of the model chosen. These models were TIP4P/Ice[14] and the six-site model[15] which have  $I_h$  melting temperatures of  $\sim 270\text{K}$  and  $\sim 289\text{K}$ [16, 17] respectively. Each model represents oxygen as a Lennard-Jones particle and hydrogen as a positive point charge. Each model also has a negative point charge located near the oxygen bisecting the HOH bond angle, referred to as the “*M*-site”. In addition to this, the six-site model, Fig. 1, also includes Lennard-Jones potentials on hydrogen atoms and “lone pairs” in the form of negative point charges. Both models were developed with the intention of simulating low temperature water and ices. Analysis of the molecular dynamics trajectories was done with software provided with GROMACS for density calculations and home-made software for other analysis such as the CHILL algorithm.

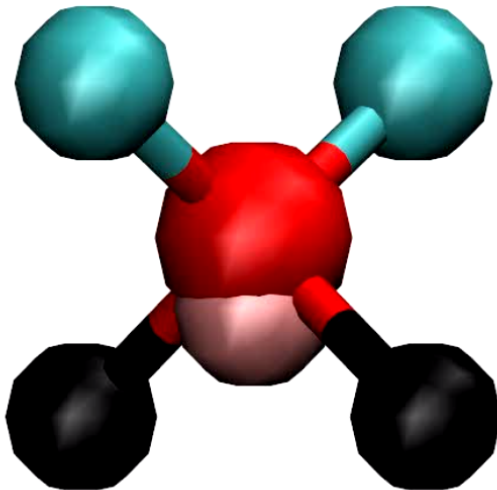


Figure 1: six-site water. Oxygen, hydrogen, *M*-site and lone pairs are red, black, pink and cyan respectively. TIP4P/Ice is similar, but lacks the lone pairs.

In the simulation cell two slabs of the crystal being studied are placed facing each other to cancel electric fields produced by the finite thickness of the slabs. The slabs meet the boundaries in such a way that the periodicity continues the crystal, and as such produces an infinite surface. Water molecules are placed between the slabs to achieve a density between 0.92 and 0.96g/mL. On the other side of the slabs a gap of 0.5 nm is left between the slab and the bottom and top of the cell. This allows the use of 3D particle mesh ewald to account for long range electrostatics in the simulation and preserve a system that is only

infinite in two dimensions. Generally the positions of the ions in the crystal are fixed and only the water molecules are allowed to move. The temperature is held at 300K for 1ns to equilibrate the system before the temperature is dropped over the course of 1ns to the simulation temperature for the remainder of the simulation. The simulation temperature is usually 20 degrees below the melting point of the water model in use for silver iodide and 30 degrees below melting for minerals.

### 3 Results and Discussion

#### 3.1 Infinite AgI Slabs

Silver iodide, a cloud seeding agent[18], is one of the best IN known[4] and can nucleate ice at temperatures as warm as -3°C. Researchers suggested that silver iodide is an effective IN due to its small lattice mismatch with ice[19]. We started research with silver iodide since it is such an effective IN and provides a case to test if a small lattice mismatch with ice is silver iodide's main reason for being an IN.

Under atmospherically relevant conditions there are two phases of silver iodide that can exist[20].  $\beta$ -AgI is the most stable phase and adopts a hexagonal wurtzite structure. A metastable phase,  $\gamma$ -AgI, also exists under atmospherically relevant conditions with both ions forming a FCC structure that has half of the tetrahedral holes filled by the counter ion. These structures are related by the  $\beta$ -AgI(0001) and  $\gamma$ -AgI(111) faces which are almost identical. Each face is made of chair conformation hexagonal rings of alternating silver and iodide ions forming a bilayer, with either all the silver or all the iodide ions occupying the upper part of the chair and the other ions below. Stacking of this bilayer in an ABAB... sequence gives  $\beta$ -AgI and an ABCABC... sequence gives  $\gamma$ -AgI. Cleavage along the bilayer or the  $\gamma$ -AgI(001) face results in either a silver or iodide exposed face depending on which ion forms the outermost part of the bilayer.

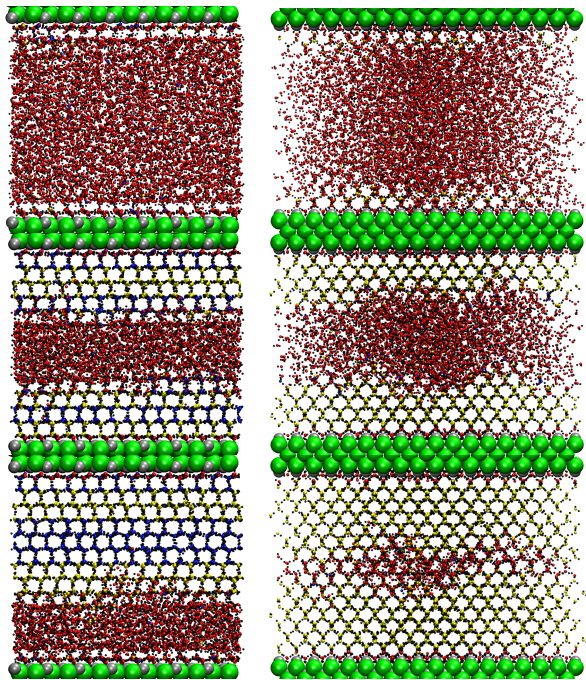


Figure 2: Several snapshots of ice growing on AgI. The left column shows growth on the silver exposed  $\beta\text{-AgI}(0001)$  face at 0, 11 and 36 ns from the time the simulation reached 270K, from top to bottom. The right column shows growth on the silver exposed  $\gamma\text{-AgI}(001)$  face at 0, 3 and 6 ns from the time the simulation reached 270K. Silver and iodide ions, hydrogen and oxygen of liquid water are silver, green, black and red respectively. Oxygen of frozen water is blue for  $I_h$  and yellow for  $I_c$ .

silver exposed  $\beta\text{-AgI}(0001)$  face was 281 K for the six-site model and 271 K for the TIP4P/Ice model. Nucleation took longer times at higher temperatures. In addition, higher nucleation temperatures may be observed if simulations were allowed to run longer.

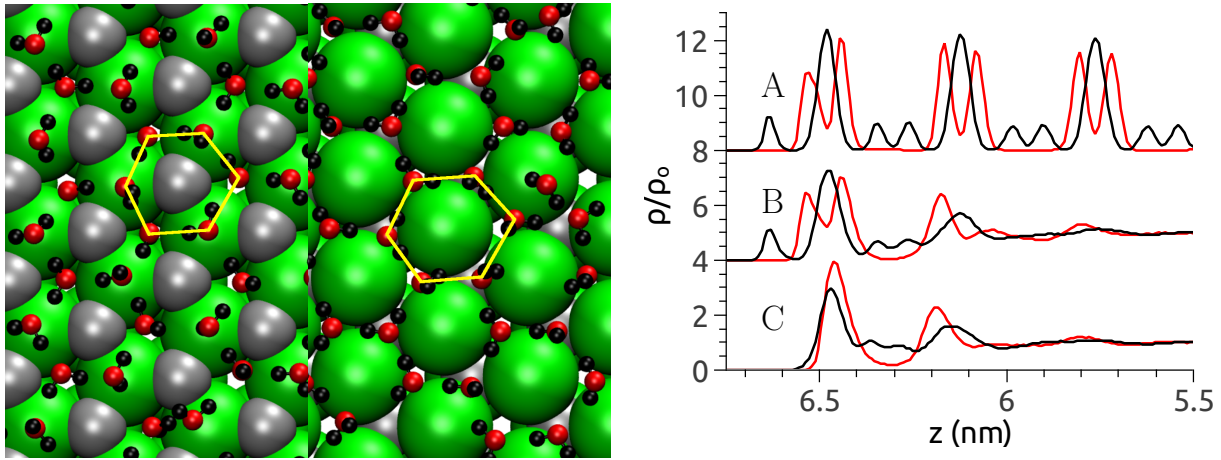
Fig. 2 displays snapshots of ice growing on the silver exposed  $\beta\text{-AgI}(0001)$  and  $\gamma\text{-AgI}(001)$  faces. The left column shows growing bilayers of ice parallel to the crystal surface. Both phases of ice are present and join with no discontinuity of the crystal other than stacking order[9]. Growth in this direction, on the  $I_h(0001)$  and  $I_c(111)$  faces, has been observed to be the preferred growth direction of ice[8]. In our simulation, crystals growing on each face

Given how similar the polymorphisms of silver iodide and ice are, several faces of silver iodide have lattice mismatches with both  $I_h$  and  $I_c$  that are less than a few percent. Of these faces the most studied theoretically is the  $\beta\text{-AgI}(0001)$  face[21, 22]. Several previous simulations have also included some of the prism faces of  $\beta\text{-AgI}$ , however, we do not know of any simulations of water on  $\gamma\text{-AgI}$ . In our simulations we simulated the silver and iodide exposed  $\beta\text{-AgI}(0001)$ ,  $\gamma\text{-AgI}(111)$  and  $\gamma\text{-AgI}(001)$  faces and the  $\beta\text{-AgI}(10\bar{1}0)$  face using potentials adapted from previous studies[23].

Ice nucleation was only observed on the silver exposed  $\beta\text{-AgI}(0001)$ ,  $\gamma\text{-AgI}(111)$  and  $\gamma\text{-AgI}(001)$  faces. Results presented below are all from simulations with the six-site model of water, however, similar results were observed for TIP4P/Ice water. The warmest temperature at which nucleation was observed on the

meet at around 11 ns with a layer of high density water between them. After meeting, the lower crystal began to melt as the upper one grew until the liquid layer reached the crystal face.

Growth on the the silver exposed  $\gamma\text{-AgI}(001)$  face is shown in the right column of Fig. 2. Almost all of the ice that was formed was cubic, and the layers of ice are oriented at an angle to the surface, not parallel. The FCC geometry of the silver iodide surface only allows cubic ice to meet the crystal favourably, therefore no  $I_h$  is formed.  $I_h$  would likely form in larger systems, as has been seen in simulations of ice nucleation with electric fields[24].

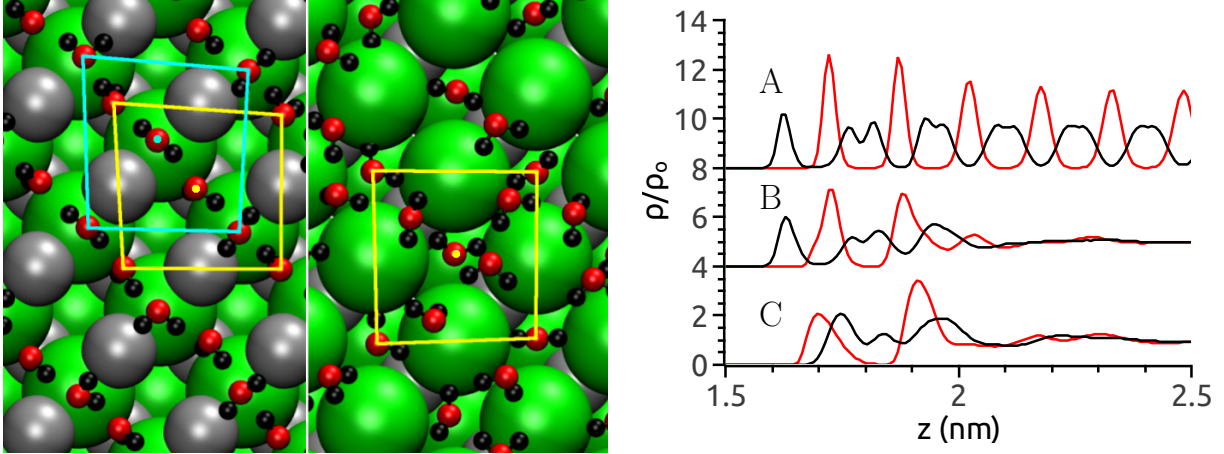


(a) The first layer of water near the silver and iodide exposed faces, left and right respectively. Silver and iodide ions, oxygen black, and hydrogen are silver, green, red and black respectively. The yellow lines highlight the hexagonal arrangement of the waters on the surface.

Figure 3: Water near the  $\beta\text{-AgI}(0001)$  face.

Both the silver and iodide exposed  $\beta\text{-AgI}(0001)$  faces organize the first layer of water into hexagonal rings, Fig. 3(a). However, the rings formed by each face are different, with the silver exposed face forming rings in the chair conformation and the iodide face forming rings that are planar. This difference is caused by the ability of the silver exposed face to accept bonding from a hydrogen of water while the iodide exposed face can not. In Fig. 3(a) some of the water molecules on the silver exposed face have one hydrogen atom, obscured below the oxygen, bonding to the surface. Bonding to the surface pulls a water molecule closer to the

silver iodide surface than the water molecules around it, and creates the chair conformation of the hexagonal rings that make up ice. This bonding may be caused by the coulombic attraction between the positive hydrogen and the negative iodide ions below the silver ions of the silver exposed face. The iodide face, in contrast, shows no hydrogen pointing toward the surface, as hydrogen is now repelled by the positive silver ions below the surface iodides.



(a) The first layer of water near the silver and iodide exposed faces, left and right respectively. Yellow highlights the FCC black, near the (A) silver exposed face at 270K, (B) 300K and face made by the first layer of water, and light blue the FCC (C) iodide exposed face at 270K. face made by the second layer of water.

Figure 4: Water near the  $\gamma\text{-AgI}(001)$  face.

The density profiles in Fig. 3(b) agree with the assessment of hydrogen atoms bonding to the silver exposed face and not bonding to the iodide exposed face. Profile A shows the density of ice near the silver iodide surface. The oxygen density shows a repeating doublet from each bilayer of ice. Hydrogen is arranged in a triplet around the doublet with the middle peak arising from hydrogen bonding within the bilayer and the outer peaks from bonding to neighbouring bilayers or silver iodide. Profile B shows the pre-freezing density profile of water on the silver exposed face and it is clear that the first layer of ice is already partially formed by interactions with the silver iodide surface. In both profiles A and B, a hydrogen peak is clearly seen directed toward the silver iodide surface, whereas the iodide exposed face shown in profile C shows no peak from hydrogens directed toward the silver iodide surface.

The surface layer of water shows that both hydrogen and oxygen remain largely as a single large peak with some hydrogen density showing bonding to water in the next layer. Monte Carlo calculations of water on  $\beta$ -AgI(0001) carried out by Shevkunov agree with our results of hydrogen interacting with the second layer of ions. He also found that the silver exposed surface has a lower energy than the iodide exposed face when water is on the surface[25].

Although a different face, the  $\gamma$ -AgI(001) surface has very similar behaviour to the  $\beta$ -AgI(0001) surface with respect to the ice nucleating ability of the silver and iodide exposed faces. The faces are from an FCC lattice, Fig. 4(a), and arrange water into a FCC pattern as is highlighted by the yellow and light blue lines and dots on the figures. Only the closest layer of water is organized on the iodide exposed face, while the organization extends beyond the first layer on the silver exposed face, Fig. 4(a). Again, hydrogen can be seen bonding to the silver exposed face, but not to the iodide exposed face, likely for the same reasons as the  $\beta$ -AgI(0001) surface: attraction or repulsion by the sub-surface ions. Density profiles in Fig. 4(b) show the density of water near the  $\gamma$ -AgI surface. Profile A is after the water has frozen into cubic ice. Oxygen gives an equally spaced repeating pattern of peaks. These peaks are from the FCC structure of  $I_c$ , which also has half the tetrahedral holes filled and form an inter-penetrating FCC lattice. The hydrogen density profile, with peaks on either side of the oxygen peak, shows that they are oriented to bond to water molecules in neighbouring layers, or to the silver iodide crystal. Before freezing, Profile B, water shows a similar density profile to ice in its first two layers as the surface organizes the water. This order is lost on the iodide face, Profile C, as the first oxygen peak is not as sharp as on the silver exposed face, and the hydrogen density shows that rather than bond to the crystal, hydrogen atoms are pointing away from it.

The lattice mismatch for both the silver and iodide exposed faces are the same, yet by changing which ion is exposed on the surface the ability of the surface to nucleate ice is created or stopped. The  $\gamma$ -AgI(111) face, due to its similarity to the  $\beta$ -AgI(0001), face shows similar behaviour. These results demonstrate that a low lattice mismatch with ice is insufficient to predict the ice nucleation behaviour of a material. To nucleate ice, the surface

must be able to organize water into an ice-like structure which likely entails the ability for hydrogen atoms to undergo bonding with the surface.

The seventh face that was simulated was the  $\beta\text{-AgI}(10\bar{1}0)$  face, Fig. 5. Compared to the  $\beta\text{-AgI}(0001)$  face, which causes water to adopt an array of chair conformed hexagonal rings,  $\beta\text{-AgI}(10\bar{1}0)$  exposes a face that was thought may be able to organize water into hexagonal rings in the boat conformation. Boat conformations appear in  $I_h$  which produces boat shaped rings between each bilayer. Lattice mismatch between each face of silver iodide and  $I_h$  is small, however, no ice was seen to nucleate on this face. We suspect that although the rings are the right size for ice, the fact that they are made of different ions with differing charges and sizes prevents a favourable match in a way that will nucleate ice.

Additional simulations were done with the  $\beta\text{-AgI}(0001)$  face with various changes to the surface and/or to the interaction parameters used. To test the effect of charge of the silver iodide model we varied the magnitude of charge given to each silver and iodide ion from  $\pm 0e-1.0e$ . Most simulations were run with charges of  $\pm 0.6e$ , however we observed ice nucleation for charges from  $\pm 0-0.8e$ , although the  $0.8e$  simulation took 473ns to nucleate. Simulations with no charge are interesting as they suggest that the atomistic roughness of the surface can be enough to nucleate ice. We also simulated a smooth 2D surface by bringing the silver and iodide ions into the same plane and varying the Lennard-Jones parameters. For the proper model parameters and when all the ions use the iodide parameters ice still nucleated, however, when all the ions used the silver parameters no ice nucleation was observed.

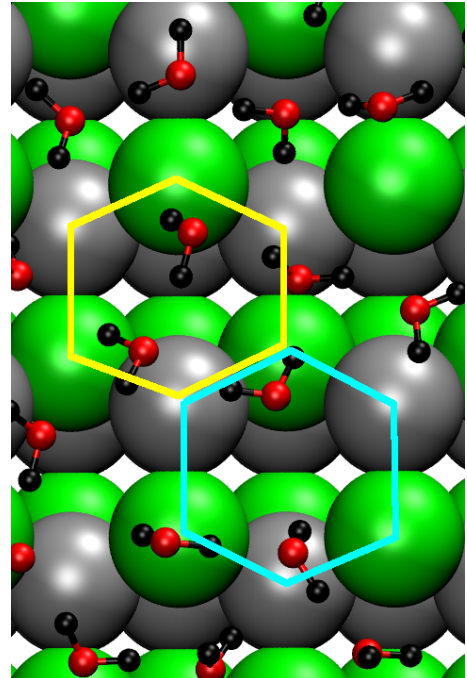


Figure 5: First layer of water near the  $\beta\text{-AgI}(10\bar{1}0)$  face. Yellow lines show a ring that is concave out of the page, and the light blue a ring that is convex.

## 3.2 Ongoing and future work

### 3.2.1 AgI Disks

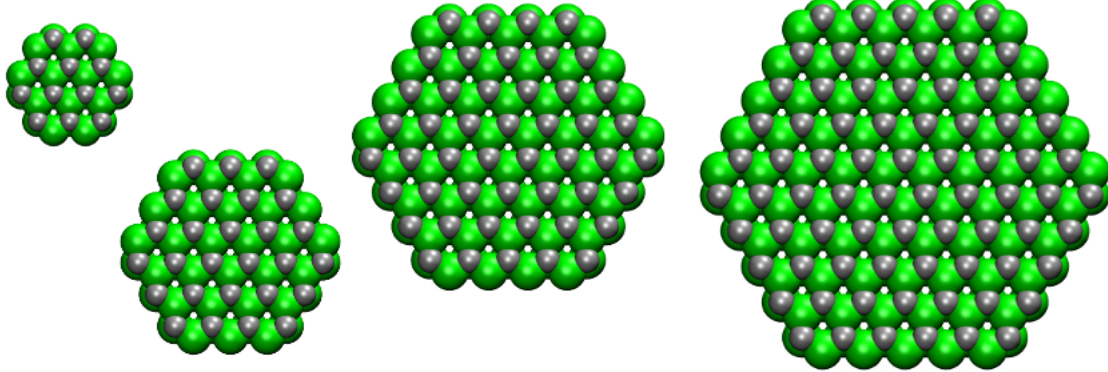


Figure 6: Hexagonal disks used in simulations. From left to right the diameters are 0.69nm, 1.15nm, 1.61nm and 2.07nm.

Having established a mechanism by which ice will nucleate on an infinite silver iodide surface we are turning our attention to the effect of the size of the slab of silver iodide. Simulations are under way with hexagonal disks showing the  $\beta\text{-AgI}(0001)$  face. We hope to establish a size and temperature dependence of ice nucleation on this surface and compare those results to classical nucleation theory[26].

To date simulations have been run on the disks pictured in Fig. 6. Three of the larger disks have produced stable clusters of ice at supercooling of 20 degrees, and the larger two disks have nucleated bulk ice when supercooled 30 degrees with the six-site model, but not with TIP4P/Ice. Fig. 7 shows clusters of ice on the 2.07nm disk.

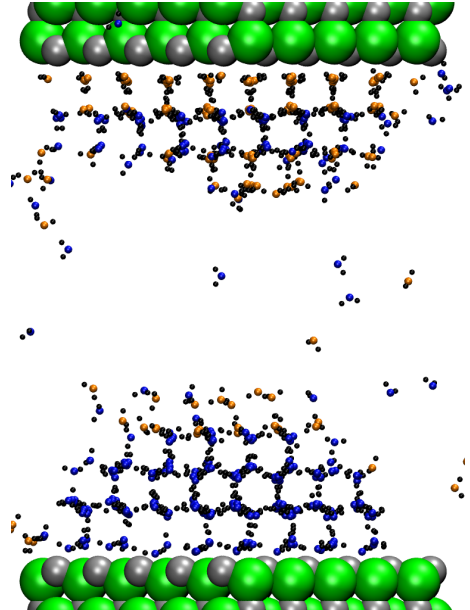


Figure 7: Clusters of ice on two facing  $\beta\text{-AgI}(0001)$  disks. Silver and iodide ions and hydrogen are silver, green and black respectively. Oxygen of hexagonal and cubic ice are blue and orange respectively.

### **3.2.2 Kaolinite and Feldspar**

Previous work by Croteau and colleagues used Grand Canonical Monte Carlo calculations to study water on the surface of the clay kaolinite[27, 28, 29, 30],  $\text{Al}_2\text{Si}_2\text{O}_5(\text{OH})_4$ . It was found that water on the clay's surface was organized into hexagonal rings, but the structure did not match that of ice. Surface defects in the form of trenches were also studied and it was found that the water was more ordered in the trenches due to electric fields generated by them. Recently, molecular dynamics simulations on kaolinite have shown that ice growth is influenced by the surface to be completely  $I_h$  with the bilayer oriented perpendicular to the kaolinite surface[31] when the system was small, but vanished as the size of the system was increased.

Thus far we have carried out simulations on two (001) faces of fixed kaolinite and observed no ice nucleation. The mentioned study[31] used kaolinite that was able to move and noted that 1/3 of the surface hydroxides where aligned parallel to the crystal face and could thus accept hydrogen bonds from water. We are now running simulations with surface hydroxides that are free to rotate and have observed ice nucleation.

Recent experimental studies on ice nucleation by clays has suggested that the feldspar family of minerals is the dominant IN of airborne clay particles[32]. Feldspar is a mixture of three structurally similar minerals that differ in their content of potassium, sodium and calcium and silicon substitution by aluminium: orthoclase  $\text{KAlSi}_3\text{O}_8$ , albite  $\text{NaAlSi}_3\text{O}_8$  and anorthite  $\text{CaAl}_2\text{Si}_2\text{O}_8$ . Of these three feldspars, orthoclase was found to be the most prolific ice nucleus. We will carry out simulations of water on these clays to determine the reason for their effectiveness in ice nucleation.

### **3.2.3 Graphite**

Recently a simulation showing ice formation on flat and curved sheets of graphene was reported[33], with decreased nucleation ability of the sheet as it was bent. These results are interesting, however, it is possible that the relatively simple mW model of water used in the simulation may be influencing the results. The mW model is a coarse grained model of

water that represents water as a neutral single point, using a 2-body potential to regulate distances between waters and a 3-body potential to order water into a tetrahedral geometry. Bulk properties of water are represented well by this model, however, it does nucleate ice very readily which may be over emphasizing the ice nucleation ability of graphene. Also the lack of hydrogen may be affecting the results, as we have observed for silver iodide, hydrogen plays a crucial role in ice nucleation. We will explore the ice nucleating ability of graphene using the atomistic models described above.

### 3.2.4 *Pseudomonas syringae*

Proteins have been observed to both nucleate ice and inhibit ice growth. Among ice nucleation proteins, one of the most effective is produced by the bacteria *Pseudomonas syringae*. The gene that produces this protein has been sequenced[34] and the corresponding protein contains 1200 amino acids with 976 of the amino acids from the mid-part of the protein showing a repeating pattern every 8, 16 and 48 amino acids. A simulation on part of the repeating section of the ice nucleation protein from *Pseudomonas borealis*, which is very similar to the protein from *Pseudomonas syringae* predicted a  $\beta$ -helix structure of that region[35]. This section localized water on its surface in spacings similar to that of  $I_h$ . They also found that the  $\beta$ -helix could dimerize and form a larger nucleation surface. We will try to perform similar simulations with the protein from *Pseudomonas syringae* and cool the simulation in an attempt to nucleate ice.

## 4 Conclusion

The aim of this project is to use molecular dynamics simulations to study ice nucleation on various atmospherically relevant IN. To date simulations have been carried out on infinite silver iodide surfaces, the simulations have shown that lattice mismatch is not sufficient to predict the ability of a material to nucleate ice, but interactions with the surface are important. Current simulations are exploring the effect of the size of the silver iodide slab needed to nucleate ice and infinite surfaces of kaolinite and feldspar. In the future we will

also explore graphite and the ice nucleation protein from *Pseudomonas syringae*.

## References

- [1] JH Seinfeld and SN Pandis. *Atmospheric chemistry and physics: from air pollution to climate change- 2ed.* Wiley-Interscience, New Jersey, 2006.
- [2] T Bartels-Rausch. Ten things we need to know about ice and snow. *Nature*, 494:27–29, 2013.
- [3] T Bartels-Rausch and et al. Ice structures, patterns, and processes: a view across the icefields. *Reviews of Modern Physics*, 84(2):885–944, 2012.
- [4] HR Pruppacher and JD Klett. *Microphysics of clouds and precipitation.* Springer, New York, 2010.
- [5] DA Hegg and MB Baker. Nucleation in the atmosphere. *Reports on Progress in Physics*, 72:056801, 2009.
- [6] G Malenkov. Liquid water and ices: understanding the structure and physical properties. *Journal of Physics: Condensed Matter*, 21:283101, 2009.
- [7] AV Brukhno, J Anwar, R Davidchack, and R Handel. Challenges in molecular simulation of homogenous ice nucleation. *Journal of Physics: Condensed Matter*, 20:494243, 2008.
- [8] MA Carignano. Formation of stacking faults during ice growth on hexagonal and cubic substrates. *The Journal of Physical Chemistry C Letters*, 111:501–504, 2007.
- [9] GP Johari. On the coexistence of cubic and hexagonal ice between 160 and 240k. *Philosophical Magazine B*, 78(4):375–383, 1998.
- [10] D Frenkel and B Smit. *Understanding Molecular Simulations.* Academic Press, San Diego, 2002.
- [11] EB Moore, E de la Llave, K Welke, DA Scherlis, and V Molinero. Freezing, melting and structure if ice in a hydrophilic nanopore. *Physical Chemistry Chemical Physics*, 12(16):4124–4134, 2010.
- [12] MP Allen and DJ Tildesley. *Computer simulations of liquids.* Oxford University Press, Oxford, 1987.
- [13] S Pronk and et al. Gromacs 4.5: a high-throughput and highly parallel open source molecular simulation toolkit. *Bioinformatics*, 29(7):845–854, 2013.
- [14] JL Abascal, E Sanz, RG Fernández, and C Vega. A potential model for the study of ices and amorphous water: Tip4p/ice. *Journal of Chemical Physics*, 122(23):234511, 2005.
- [15] H Nada and JPJM van der Earden. An intermolecular potential model for the simulation of ice and water near the melting point: a six-site model of h<sub>2</sub>o. *Journal of Chemical Physics*, 118(16):7401–7413, 2003.

- [16] JLF Abascal, RG Fernández, C Vega, and MA Carignano. The melting temperature of the six site potential model of water. *Journal of Chemical Physics*, 125:166101, 2006.
- [17] RG Fernández, JLF Abascal, and C Vega. The melting point of ice  $i_h$  for common water models calculated from direct coexistence of the solid-liquid interface. *The Journal of Chemical Physics*, 124:144506, 2006.
- [18] RT Bruninjes. A review of cloud seeding experiments to enhance precipitation and some new prospects. *Bulletin of the American Meteorological Society*, 80(5):805–820, 1999.
- [19] B Vonneget. The nucleation of ice formation by silver iodide. *Journal of Applied Physics*, 18(7):593–595, 1947.
- [20] N Hull and DA Keen. Pressure-induced phase transitions in agcl, agbr and agi. *Physical Review B*, 59(2):750–761, 1999.
- [21] JH Taylor and BN Hale. Monte carlo simulations of water-ice layers on a model silver iodide substrate: a comparison with bulk ice systems. *Physical Review B*, 47(15):9732–9741, 1993.
- [22] SV Shevkunov. Adsorption of water vapor on the agi surface: a computer experiment. *Russian Journal of General Chemistry*, 75(10):1632–1642, 2005.
- [23] BN Hale and J Kiefer. Studies of  $h_2o$  on  $\beta$ -agi surfaces: an effective pair potential model. *The Journal of Chemical Physics*, 73(2):923–933, 1980.
- [24] JY Yan and GN Patey. Ice nucleation by electric surface fields of varying range and geometry. *The Journal of Chemical Physics*, 139:144501, 2013.
- [25] SV Shevkunov. Structure of water in microscopic fractures of a silver iodide crystal. *Russian Journal of Physical Chemistry*, 88(2):313–319, 2014.
- [26] NH Fletcher. Nucleation by crystalline particles. *The Journal of Chemical Physics*, 38(1):237–240, 1963.
- [27] T Croteau, AK Bertram, and GN Patey. Adsorption and structure of water on kaolinite surfaces: possible insight into ice nucleation from grand canonical monte carlo calculations. *The Journal of Physical Chemistry A Letters*, 112(43):10708–10712, 2008.
- [28] T Croteau, AK Bertram, and GN Patey. Simulation of water adsorption on kaolinite under atmospheric conditions. *The Journal of Physical Chemistry A*, 113(27):7826–7833, 2009.
- [29] T Croteau, AK Bertram, and GN Patey. Water adsorption on kaolinite surfaces containing trenches. *The Journal of Physical Chemistry A*, 114(5):2171–2178, 2010.
- [30] T Croteau, AK Bertram, and GN Patey. Observations of high-density ferroelectric ordered water in kaolinite trenches using monte carlo simulations. *The Journal of Physical Chemistry*, 114(32):8396–8405, 2010.
- [31] SJ Cox, Z Raza, SM Kathmann, B Slater, and A Michaelides. The microscopic features of heterogeneous ice nucleation may affect the macroscopic morphology of atmospheric ice crystals. *Faraday Discussions*, 167:389–403, 2013.

- [32] JD Atkinson and et all. The importance of feldspar for ice nucleation by mineral dust in mixed-phase clouds. *Nature*, published online: June:–, 2013.
- [33] L Lupi, A Hudait, and V Molinero. Heterogeneous nucleation of ice on carbon surfaces. *Journal of the American Chemical Society*, pages –, 2014.
- [34] RL Green and GJ Warren. Physical and functional repetition in a bacterial ice nucleation gene. *Nature*, 317:645–648, 1985.
- [35] CP Garnham, RL Campbell, VK Walker, and PL Davis. Novel dimeric  $\beta$ -helical model of an ice nucleation protein with bridged active sites. *BMC Structural Biology*, 11:36, 2011.